THE JOURNAL OF BIOLOGICAL CHEMISTRY
© 1990 by The American Society for Biochemistry and Molecular Biology, Inc.

Vol. 265, No. 35, Issue of December 15, pp. 21561-21566, 1990
Printed in U.S.A.

Type II Regulatory Subunit Dimerization Determines the Subcellular Localization of the cAMP-dependent Protein Kinase*

(Received for publication, July 9, 1990)

John D. Scott‡§¶, Renata E. Stofko‡, J. Randy McDonald§, Jeffrey D. Comer‡, Elizabeth A. Vitalis‖, and Jo Ann Mangili‖

From the ‡Vollum Institute for Advanced Biomedical Research, L474, Portland, Oregon, 97201, the §Department of Biochemistry and Molecular Biology, Oregon Health Sciences University, Portland, Oregon, 97201, and the ‖Department of Physiology and Biophysics, University of California Irvine, MED SCI I, D340, Irvine, California 92717

The type II cAMP-dependent protein kinase (PKA) is localized to specific subcellular environments through binding of dimeric regulatory subunits (RII) to anchoring proteins. Cytoskeletal localization occurs through RII dimer interaction with the PKA substrate molecule microtubule-associated protein 2 (MAP2). RIIα deletion mutants and RIIα/endonexin chimeras retained MAP2 binding activity if they contained the first 79 residues of the molecule. Disruption of RIIα dimerization always prevented MAP2 interaction because 1) RIIΔ 1–14 (an amino-terminal deletion mutant lacking residues 1–14) was unable to bind MAP2 or form dimers, and 2) a modified RIIα monomer including residues 1–14 did not bind MAP2. Chimeric proteins containing the first 30 residues of RIIα fused to endonexin II formed dimers but did not bind MAP2. This suggested other side-chains between residues 30–79 also participate in MAP2 interaction. Peptide studies indicate additional contact with MAP2 may occur through an acidic region (residues 68–82) close to the RII autoinhibitor domain. Therefore, anchored PKA holoenzyme topology may position the catalytic subunit and MAP2 as to allow its preferential phosphorylation upon kinase activation.

Most cAMP-responsive events are triggered through phosphorylation of proteins by the cAMP-dependent protein kinase (PKA).[1] Ligand-receptor interactions, coupled to G-proteins, transduce extracellular signals through the membrane stimulating adenylate cyclase on the inner membrane surface (1). This elevates intracellular cAMP causing PKA activation (2). Four molecules of cAMP bind each dormant PKA holoenzyme causing release of two active catalytic (C) subunits from the regulatory (R) subunit dimer (3). Phosphorylation of substrate proteins triggers individual cellular responses. Therefore, the site of PKA activation may determine which cAMP-mediated event is triggered.

Subcellular fractionation and immunochemical localization detect PKA in particulate and membrane fractions (4, 5). Subcellular localization of PKA is directed through the R subunit (6). Two R subunit classes exist, RI and RII, which form type I and II holoenzymes, respectively (7, 8). Two distinct isoforms of RI and of RII have been identified and their genes isolated (9–12). Both RI isoforms are primarily cytoplasmic while up to 75% of either RII isoform is localized on membranes, subcellular organelles, or the cytoskeleton (4, 5, 13). In the brain both RII isoforms (RIIα and RIIβ) are localized through interaction with specific anchoring proteins (14, 15). Using RIIα as an affinity ligand, several proteins were purified from crude tissue extracts. Most of these molecules were hyperphosphorylated in response to cAMP (16).

Cytoskeletal attachment of type II PKA occurs through interactions between RII and microtubule-associated protein 2 (MAP2) (17). The site on MAP2 which contacts RII has been localized to a 31-residue peptide (18, 19). This report documents characterization of the MAP2 receptor site on murine RIIα. Using RII deletion mutants and peptide probes, we have identified two distinct peptide components of the MAP2 receptor. The first 30 residues promote R/R dimerization which is necessary for MAP2 interaction. Additional MAP2 contact may be provided by acidic clusters, 40 residues downstream on each RII protomer. A survey of other anchoring proteins suggests all bind at the same or overlapping sites on RII.

EXPERIMENTAL PROCEDURES

Purification of Proteins and Peptides—Bovine and murine MAP2 were purified by the taxol method of Vallee (20). Bovine RIIα and C subunit were gifts from Dr. Erwin Reimann (Medical College of Ohio) and p47, an RII-binding fragment of the bovine p75 protein was graciously provided by Dr. Charles Rubin (Albert Einstein College of Medicine). Bovine testis casein kinase II and the peptide Lys-Tyr-Ile-Leu-Asp-Asp-Leu-Glu-Pro-Asp-Glu Glu-Leu-Glu-Asp was generously provided by Dr. David Lichfield (University of Washington). Synthetic peptides were synthesized by the Vollum Institute peptide facility.

RII Overlay Procedure—This was performed by the method of Lohman and colleagues (16) with modifications documented by Bergman *et al.* (15).

Quantitative MAP2 Binding—Quantitative MAP2/RII binding was measured by counting ^{32}P-RIIα bound to immobilized MAP2. Aliquots of purified RIIα or the appropriate deletion mutant (2 mg) were phosphorylated with bovine testis casein kinase II (50 nM) in 20 μl of 50 mM Tris buffer, pH 7.5, 10 mM MgAc 150 mM NaCl, 5 μM [^{32}P] ATP (specific activity 6000 Ci/mmol) at 30 °C for 1 h. Samples were desalted on Sephadex G-25 minicolumns before the protein concentration and ^{32}P incorporation were determined. The stoichiometry of ^{32}P incorporation was 1.69 ± 0.12 mol/mol RIIα monomer (n = 18). RIIα (50 μg) aliquots in Tris-buffered saline, pH 7.5, 5% (w/v) powdered milk, 0.1% (w/v) bovine serum albumin (1 ml) were incubated for 4 h at room temperature with individual 1 cm^2 nitrocellulose squares containing 5 μg of purified bovine MAP2 (5 μl) adsorbed onto their surface. After incubation each filter was individually washed (6

* This work was supported by the National Institute of General Medicine Grant GM 44427 and Medical Research Foundation Grant MRF 396-521. The costs of publication of this article were defrayed in part by the payment of page charges. This article must therefore be hereby marked "*advertisement*" in accordance with 18 U.S.C. Section 1734 solely to indicate this fact.

¶ To whom correspondence should be addressed.

[1] The abbreviations used are: PKA, cAMP-dependent protein kinase; HPLC, high pressure liquid chromatography; Mes, 4-morpholineethanesulfonic acid; SDS, sodium dodecyl sulfate; MAP2, microtubule-associated protein 2.

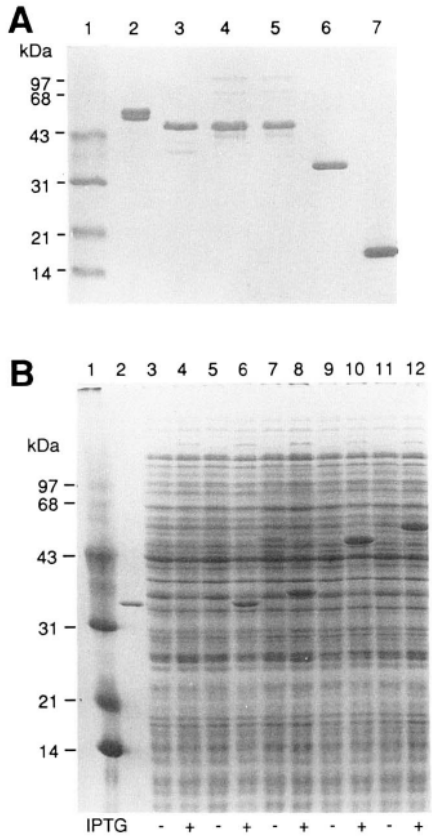

FIG. 1. **Analysis of recombinant RIIα proteins.** Murine RIIα (10 μg) and various deletion mutants (*A*), and bacterial extracts from cells expressing each RII/endonexin chimera were analyzed by SDS-gel electrophoresis on a 12% (w/v) polyacrylamide gel. *A*, shows the purity of each recombinant RIIα protein as assessed by SDS-gel electrophoresis, molecular weight markers (*lane 1*), RIIα (*lane 2*), RIIΔ 1–14 (*lane 3*), RIIΔ 1–30 (*lane 4*), RIIΔ 1–35 (*lane 5*), RIIΔ 248–400 (*lane 6*), RIIΔ 128–400 (*lane 7*). Molecular mass markers were phosphorylase *b* (97 kDa), bovine serum albumin (66 kDa), ovalbumin (43 kDa), carbonic anhydrase (31 kDa), soya bean trypsin inhibitor (21.5 kDa) and lysozyme (14.4 kDa). *B*, shows levels of expression of RII/endonexin constructs in plasmid pEt 11d, molecular weight markers (*lane 1*), endonexin II (*lane 2*), control plasmid (*lanes 3* and *4*), RII 1–14/endonexin (*lanes 5* and *6*), RII 1–30/endonexin (*lanes 7* and *8*), RII 1–79/endonexin (*lanes 9* and *10*), RII 1–115/endonexin (*lanes 11* and *12*). *Lanes 3, 5, 7, 9,* and *11* contain bacterial extracts grown without (−) isopropyl-1-thio-β-D-galactopyranoside (*IPTG*) while lanes *4, 6, 8, 10,* and *12* contain bacterial extracts grown with (+)isopropyl-1-thio-β-D-galactopyranoside.

× 10 min) in Tris-buffered saline, pH 7.5, 0.1% Tween 20 at room temperature. Each filter was dried before immersion in scintillation fluid, and the nitrocellulose was allowed to dissolve before measurement by liquid scintillation counting.

RII 68–82 peptide was phosphorylated with 5 μM [^{32}P]ATP (specific activity 1000 cpm/nM) by casein kinase II as described above. Phosphopeptide was separated from unreacted [^{32}P]ATP by reverse-phase HPLC using a Vydac RP-P C18 column equilibrated in 0.1% (w/v) trifluoroacetic acid with a linear gradient of 0–40% acetonitrile.

Construction of RIIα Expression Plasmid pTRC RII—All truncated RIIα proteins were expressed in *Escherichia coli* JM 109 using a modified pTRC/pUC 19 vector system. The TRC promoter was excised from the bacterial plasmid pKK 233-2 by digestion with *Bam*HI and *Nco*I. This 300-base pair *Bam*HI/*Nco*I fragment and an oligonucleotide linker with *Nco*I and *Pst*I ends, representing the first 47 bases of murine RIIα was ligated into pUC 19 (*Bam*HI/*Pst*I cut). This plasmid was amplified in bacteria before a subsequent aliquot was used to construct the RIIα expression plasmid *pTRC RII* by inserting a 1.5-kilobase *Pst*I/*Eco*RI fragment containing the remainder of the murine RIIα coding sequence behind the oligonucleotide linker.

Construction of RII Deletion Mutants—Defined segments of 5′-coding sequence were removed by restriction digestion of pTRC RII, the murine RIIα expression vector (Fig. 2*B*). Linearized vectors (500 ng) were ligated to *Nco*I linkers (CC**ATG**G) by incubation for 4 h at room temperature with T_4 DNA ligase (10 units) in Ligase buffer (both Bethesda Research Laboratories) to final volume of 10 μl. This created an in frame translational start site at the new 5′ end of the RIIα coding region (Fig. 2*B*). Each vector was digested with excess *Nco*I (50 units) to remove extraneous DNA between the new start codon and the pTRC promoter. After purification each fragment was ligated to reform the circular DNA with T_4 DNA ligase (10 units) in Ligase buffer (both Bethesda Research Laboratories) to final volume of 10 μl for 16 h at 15 °C.

RIIα proteins truncated in the carboxyl-terminus were constructed by similar procedures. Plasmid pTRC RII was digested with the appropriate restriction enzyme to remove defined segments of 3′-coding sequence (Fig. 1*B*). All overhanging DNA ends were filled-in by Klenow or removed by T_4 polymerase. Then a 12-base pair translational terminator (GCT**TAATTAA**GC) was ligated in frame at the 3′ end to provide a stop codon. The nomenclature for each deletion protein was devised to indicate the residue number of the deletion site in the murine RIIα protein sequence (*e.g.* RIIΔ 1–14, an amino-terminal deletion removing residues 1–14).

Purification of Recombinant RII Proteins—All recombinant RIIα proteins with the exception of RIIΔ 128–400 were purified to homogeneity by affinity chromatography on cAMP-Sepharose by the method of Weber *et al.* (21).

Two liters of LB broth, 50 μg/ml ampicillin were inoculated with an overnight culture (1 ml) of RIIα expressing *E. coli*. The cells were grown by shaking at 37 °C until the OD_{550nm}, was 0.300. Maximal RIIα expression was induced by the addition of 1 mM isopropyl-1-thio-β-D-galactopyranoside, and the cells were grown for a further 4 h to allow accumulation of the protein. At this time bacteria were concentrated by centrifugation (3,000 rpm) for 10 min at 4 °C and resuspended in 25 mls of lysis buffer (50 mM Mes, pH 6.8, 150 mM NaCl, 15 mM β-mercaptoethanol, 1 μg/ml leupeptin, 1 μg/ml pepstatin, 50 mM benzamidine). Bacterial lysis was achieved by two passages through a French press. The resulting bacterial extracts were diluted to 50 ml in lysis buffer and soluble proteins (approximately 35 ml) were separated from particulate material by centrifugation (12,000 rpm) for 30 min at 4 °C. DNase 1 (1 μg/ml) was added to reduce the viscosity of the soluble bacterial extract. Soluble protein extracts were incubated with cAMP-Sepharose for 48 h at 4 °C on a rotary mixer. All preceding steps in the purifications were as described by Weber *et al.* (21). The purity of each recombinant RII protein was assessed by SDS-polyacrylamide gel electrophoresis as indicated in Fig. 1*A*.

RIIΔ 128–400 lacked both cAMP-binding domains and was refractory to cAMP-Sepharose. Partial purification was achieved by gel-filtration chromatography on a column (1.5 × 90 cm) of Sephacryl S-200 equilibrated in Tris-buffered saline, pH 7.5, 50 mM benzamidine, 1 μg/ml pepstatin, 1 μg/ml leupeptin, 50 mM benzamidine (Fig. 1*A*).

Construction of Chimeric RII/Endonexin II Proteins—Endonexin II was chosen as the carrier molecule because it exists as a monomer and bioactive protein can be recovered from bacteria. Furthermore, high titre antibodies have been raised to the protein (22, 23) which could be used to detect the chimeras using the overlay procedure. Plasmid pKK endo (pKK233-2 with the endonexin-coding region) was cut with *Nco*I at the endonexin start codon and the cohesive ends were filled in with Klenow. Linearized plasmid was further digested with *Bgl*II liberating a 1.3-kilobase DNA insert which included the complete endonexin-coding region, stop codon, and some 3′-untranslated sequences. The endonexin insert was ligated into plasmid pTRC RII where bases 42–834, 89–834, 237–834, and 345–834 of the coding region had been removed. The nucleotide sequence of each new plasmid was determined. These DNA manipulations created plasmids which expressed chimeric proteins containing the first 14, 30, 79, and 115 residues of RIIα fused to endonexin.

Higher levels of expression were achieved using the T_7 polymerase system of Studier. Each chimeric fragment (*Nco*I/*Bgl*II cut) was ligated into expression vector pET 11d. Colonies expressing chimeric proteins were detected with anti-endonexin anti-sera. Soluble protein extracts containing individual RII/endonexin chimeras were prepared as described above for recombinant RII proteins. The concentration of each RII/endonexin fraction was estimated as a percentage of the extract (10%) determined by SDS-polyacrylamide gel electrophoresis (Fig. 1*B*).

Partial Proteolysis of RII—Murine RIIα (10 mg) radiolabeled by phosphorylation with casein kinase II and 5 μM [^{32}P]ATP (specific activity 6000 Ci/mmol) was treated with trypsin (0.1 mg) for 5 min at 30 °C before the addition of 50 mM benzamidine. Two RIIα

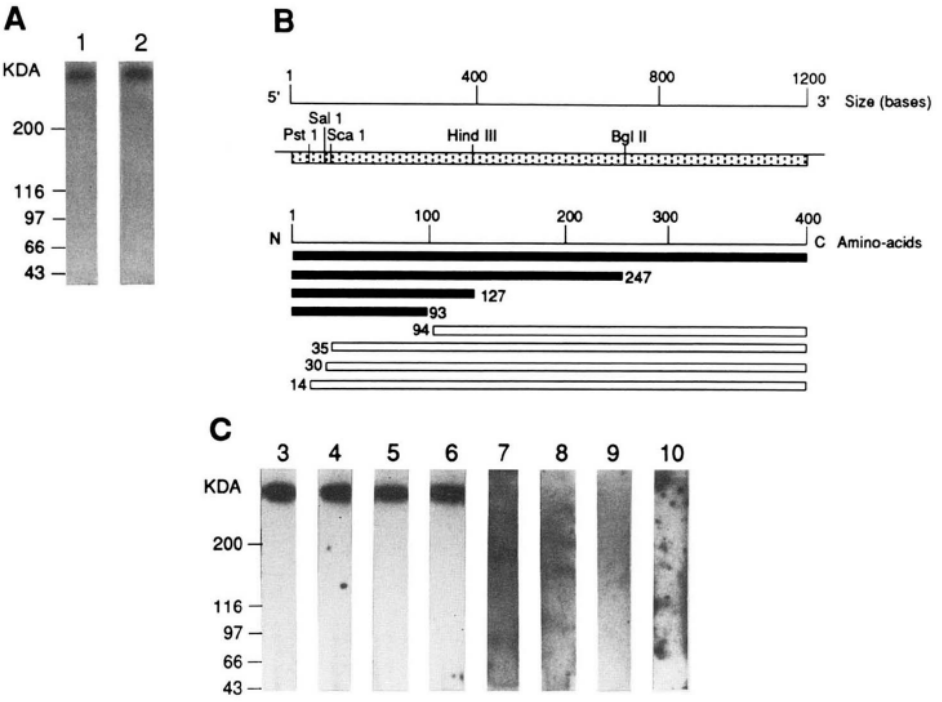

FIG. 2. **Defining the minimum RII structural requirements for MAP2 interaction.** Murine RIIα and various deletion mutants were analyzed for solid-phase MAP2 interaction. MAP2 (10 μg) was separated by gel electrophoresis on a 5% (w/v) SDS-polyacrylamide gel before electrotransfer onto nitrocellulose filters. Individual strips of filter containing single gel lanes were incubated with ^{32}P-RIIα or the appropriate RII deletion mutant using a modified protein overlay procedure (16). *A*, compares the binding characteristics of bovine RIIα (*lane 1*) and recombinant murine RIIα (*lane 2*). Molecular mass markers were myosin (200 kDa), β-galactosidase (116 kDa), phosphorylase *b* (97 kDa), and bovine serum albumin (66 kDa). *B*, outlines the construction of RIIα deletion mutants and their MAP2-binding properties. The position and name of each unique restriction site used to construct deletions is indicated. The design of each construct has been described under "Experimental Methods." Those RIIα proteins able to interact with MAP2 are indicated in *filled bars* while those refractory to MAP2 are portrayed with *open bars*. The residue number of the RIIα protein sequence where each deletion was created is indicated. *C*, shows MAP2 binding characteristics of individual RIIα deletion mutants, murine RIIα (*lane 3*), RIIΔ 246–400 (*lane 4*), RIIΔ 128–400 (*lane 5*), RIIΔ 94–400 (*lane 6*), RIIΔ 1–93* (*lane 7*), RIIΔ 1–35 (*lane 8*), RIIΔ 1–30 (*lane 9*), and RIIΔ 1–14 (*lane 10*). *Lanes 3–6* represent autoradiograph exposures of 12 h while *lanes 7–10* were exposed for 48 h. (*)RIIΔ 1–93 lacked any phosphorylation sites and was labeled with [^{32}P]N8-azido cAMP to allow detection.

TABLE I

Quantitative binding of RIIα and MAP2

The stoichiometry of RII/MAP2 interaction was determined using a quantitative binding assay (22). Phosphorylated RIIα and selected deletion mutants were used as probes (20). The stoichiometry of interaction was calculated as moles of RII/mole of MAP2, and (*) indicates monomeric RII species as assessed by gel filtration. (In all experiments minimum $n = 8$).

Sample	Stoichiometry of interaction MAP2
RII	0.91 mol/mol ± 0.23 $n = 9$
RIIΔ 1–14	0.05 mol/mol ± 0.03 $n = 9$
RIIΔ 1–35	0.08 mol/mol ± 0.02 $n = 9$
RII and 50–62 peptide (100 μM)	0.81 mol/mol ± 0.15 $n = 8$
RII and 68–82 peptide (100 μM)	0.36 mol/mol ± 0.13 $n = 9$

fragments of apparent molecular weights of 16,000 and 37,000 were detected by SDS-polyacrylamide gel electrophoresis. These fragments were separated by gel filtration on a column (1.5 × 90 cm) of Sephacryl S-200 equilibrated in 50 mM Tris-buffered saline, 1 μg/ml pepstatin, 1 μg/ml leupeptin, 50 mM benzamidine. Automated sequence analysis of the 16,000-kDa fragment yielded the sequence Gly-His-Ile-Gln-Ile-Pro the first residues of recombinant RII$\alpha_{(1)}$. Automated sequence analysis of the 37,000-kDa fragment yielded the sequence Val-Ser-Val-Xaa-Ala-Glu-Thr-Phe-Asn-Pro. This sequence corresponded to residues 94–103 of murine RIIα confirming that cleavage occurred after arginine 93 in the protein. No amino acid was assigned to position four in the sequence and is consistent with the location of cysteine 97 which could not be detected by the HPLC separation methods used. The 37,000-kDa fragment was radiolabeled with [^{32}P] azido cAMP by the method of Kerlavage and Taylor (24).

Urea Treatment of RIIα—Denatured ^{32}P-RIIα (2 mg) in 8 M urea was mixed with 1,000-fold molar excess of RII 1–14 peptide. The mixture was renatured by desalting on a gel filtration column (1.5 × 90 cm) of Sephacryl S-200 equilibrated in 50 mM Tris-buffered saline, 1 μg/ml pepstatin, 1 μg/ml leupeptin, 50 mM benzamidine. A RII 1–14 peptide hybrid was isolated with an apparent molecular weight of 50,000. In the absence of cAMP this molecule was unstable and precipitated if stored overnight at 4 °C. The hybrid RII monomer was stable for up to 7 days if stored in 10 μM cAMP and 1 mM RII 1–14 peptide at 4 °C.

Miscellaneous Methods—The nucleotide sequence of all cDNA constructs were analyzed as determined by the method of Sanger *et al.* (25). Analysis by SDS-polyacrylamide gel electrophoresis was performed by the method of Laemmli (26). Electrotransfer of proteins onto nitrocellulose was as described by Towbin and colleagues (27). Secondary structure predictions were generated for the first 100 residues of RIIα and RIIβ using the methods of Chou and Fasman (28) and Robinson and Suzuki (29). A survey of protein secondary structure motifs found in known crystal structures was as described following the procedure of Millar (30).

RESULTS

MAP2 binding was monitored by solid-phase protein blotting and confirmed that recombinant murine RIIα had similar binding characteristics as bovine heart RIIα (Fig. 2*A*). Excess recombinant RIIα (100-fold molar) blocked ^{32}P-labeled bovine RII/MAP2 interaction while an equivalent amount of rabbit

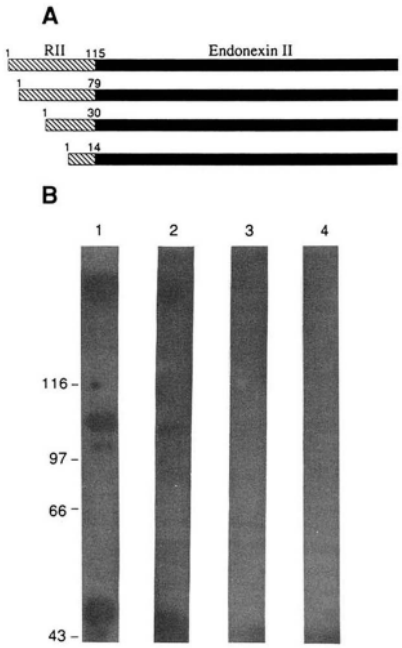

FIG. 3. **MAP2 binding characteristics of RII/endonexin II chimeras.** Chimeric proteins containing 14, 30, 79, and 115 residues of RIIα sequence fused to endonexin II were constructed as described under "Experimental Procedures." *A* is a schematic representation of each chimeric construct. *Cross-hatched box* represents RIIα sequence and the *closed box* denotes endonexin II. The number of RIIα residues in each chimera are indicated. *B* shows MAP2 binding characteristics of individual RII/endonexin chimeras. Crude microtubule extracts (15 μg) were separated by gel electrophoresis on a 5% (w/v) SDS-polyacrylamide gel before electrotransfer onto nitrocellulose filters. Individual strips of filter containing single gel lanes were incubated with each chimera (10 μg). MAP2-chimera complexes were detected with anti-endonexin antisera and ^{125}I-protein A (specific activity 5600 μCi/mM). *Lane 1* (RII 1–115/endonexin II), *lane 2* (RII 1–79/endonexin), *lane 3* (RII 1–30/endonexin), *lane 4*, endonexin. Molecular weight markers were β-galactosidase (116 kDa), phosphorylase *b* (97 kDa), bovine serum albumin (66 kDa), and ovalbumin (43 kDa). Additional RIIα-reactive bands in *lanes 1* and *2* represent unidentified RII anchoring proteins present in crude microtubule extracts.

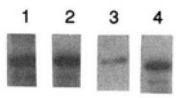

FIG. 4. **Analysis of murine RIIα-derived synthetic peptides as antagonists of MAP2 interaction.** Three synthetic peptides derived from specific regions of RIIα were analyzed for inhibition of RII/MAP2 interaction. Each peptide (100 μM) was mixed with [^{32}P] murine RIIα and incubated with MAP2 nitrocellulose filters as previously described under "Experimental Procedures." *Lane 1* represents [^{32}P]RIIα (10^6 cpm/ml) with RII 1–14 peptide SHIQIPPGLTELLQ, *lane 2* with RII 50–62 peptide IVSPTTFHTQESS, *lane 3* with RII 68–82 peptide EEDGESDSDSEDAL, and *lane 4*, control peptide KYILDDLEPEELED.

skeletal muscle RI did not. Quantitation of binding was achieved by measuring MAP2 interaction with ^{32}P-radiolabeled RIIα of known specific activity. The stoichiometry of interaction was calculated as 0.91 ($n = 9$) mol of RIIα dimer/MAP2 molecule (Table I). Binding reached a plateau in 4 h at either 22 or 37 °C (data not shown).

Deletion of Carboxyl-terminal Regions—In order to establish the minimum region of RIIα required to bind MAP2, a family of RIIα deletion mutants were constructed (Fig. 2*B*) and expressed in *E. coli*. A nomenclature defining each deletion mutant is described under "Experimental Procedures." Carboxyl-terminal deleted mutants, terminating at residues 247

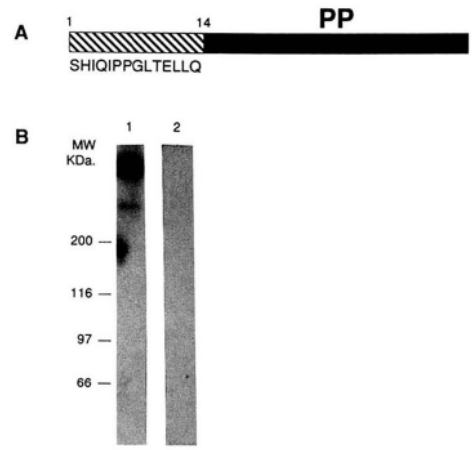

FIG. 5. **Requirement of dimerization for MAP2 interaction.** Murine RIIα was denatured with urea (8 M) and prevented from renaturing as a dimer by the addition of excess RII 1–14 peptide. RII monomers were separated by gel filtration chromatography and stabilized by storage in the presence of excess RII 1–14 peptide and cAMP. The dimeric RIIα and the modified RII monomer were analyzed for MAP2-binding properties. *A*, a schematic representation of the RII monomeric protein. *Diagonal stripes* represent putative interaction site between RII 1–14 peptide and RII protein. Phosphorylation sites for casein kinase II are indicated (*P*). *B*, interaction of dimeric RIIα and RII monomeric protein. MAP2 nitrocellulose filters were prepared as previously described and overlay procedure was as documented. *Lane 1* represents overlay with dimeric [^{32}P-RIIα (10^6 cpm/ml)] while *lane 2* represents overlay with monomeric [^{32}PRII (10^6 cpm/ml)].

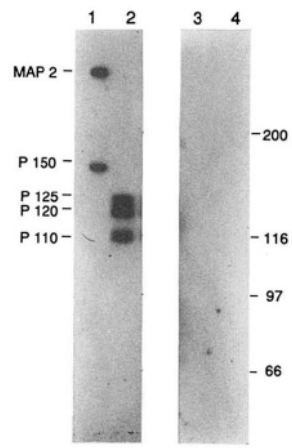

FIG. 6. **Comparison RIIα and RIIΔ 1–14 interaction with other RII-anchoring proteins.** Tissue extracts containing RII-anchoring proteins were separated by SDS-gel electrophoresis on a 4% acrylamide gel and electrotransferred to nitrocellulose filters. Overlay blots were performed using ^{32}P-RIIα (10^6 cpm/ml) as a probe (*lanes 1* and *2*) and ^{32}P-RIIΔ 1–14 (10^6 cpm/ml) as a probe (*lanes 3* and *4*). *Lanes 1* and *3* contain rat brain membrane extracts (15 μg) enriched with 5 μg/ml MAP2, and *lanes 2* and *4* bovine sperm extracts (20 μg). Sperm extracts were isolated as described (36). Relative molecular weights of the RII-anchoring proteins are indicated. Molecular weight markers are as described for Fig. 1.

and 127 bound MAP2 (Fig. 2*C*). Limited tryptic digestion of RII yields two fragments, an amino-terminal dimer (apparent molecular weight 16,000) and monomeric 37,000-kDa fragments containing both cAMP-binding domains (31). Both fragments were purified by gel filtration chromatography and protein sequence analysis confirmed cleavage occurred after arginine 93. Only the amino-terminal fragment (residues 1–93) bound MAP2 (Fig. 2*C*). Chimeric proteins (Fig. 3*A*) with residues 1–115 or 1–79 of RII fused to the carrier molecule endonexin II bound MAP2 (Fig. 3*B*). In summary only resi-

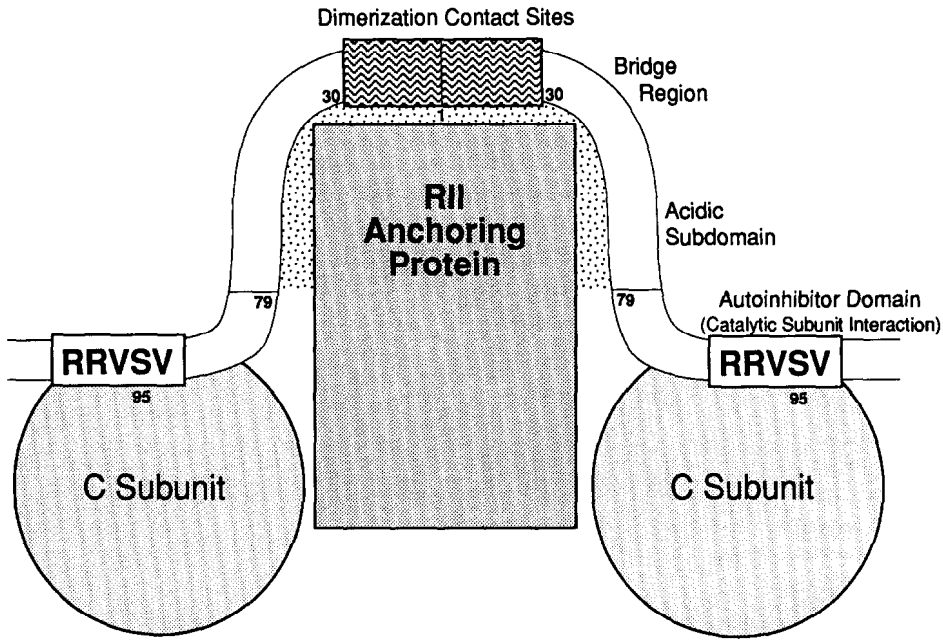

FIG. 7. **Model for RII-anchoring protein receptor site.** This schematic summarizes the findings of this report and shows how the first 79 residues of murine RIIα could interact with an RII-anchoring protein and thereby target the type II PKA holoenzyme to specific subcellular locations. *Stippled areas* represent potential sites of RII-anchoring protein interaction. The boundaries of the peptide subdomains characterized in this study are indicated as are the three putative functional regions within the RII-anchoring protein receptor site.

dues 1–79 of RII are required for MAP2 interaction.

Deletion of Amino-terminal Regions—RII mutants lacking the first 14, 30, or 35 residues were unable to bind MAP2 (Fig. 2*C*). Gel filtration of RIIΔ 1–14 revealed it was a monomer of 41,000 kDa but still bound cAMP and C subunit (data not shown). Conceivably, residues 1–14 could participate in both RII dimerization and MAP2 interaction. To establish if MAP2 interaction was mediated only through residues 1–14 of RIIα chimeric proteins were engineered. Residues 1–14 or 1–30 of RII were fused to a carrier molecule endonexin II. Neither RII 1–14/endonexin or RII 1 to 30/endotoxin bound MAP2 (Fig. 3*B*). This was confirmed by studies with a peptide corresponding to amino acids 1–14 of RII (Ser-His-Ile-Gln-Ile-Pro-Pro-Gly-Leu-Thr-Glu-Leu-Leu-Gln) which could not block RII/MAP interaction in solutions with concentrations ranging from 1 nM to 10 mM (Fig. 4 and Table I).

Requirement of RII Dimerization and Residues 30–79—Gel filtration of RII 1–30/endonexin revealed that it was dimeric, showing that residues 1–30 promote dimerization if removed from the rest of RIIα. This finding suggested additional side-chains located between residues 30–79 participate in MAP2 binding. To identify other potential MAP2-binding regions peptides corresponding to residues 50–62 (Ile-Val-Ser-Pro-Thr-Thr-Phe-His-Thr-Gln-Glu-Ser-Ser) and 68–82 (Glu-Glu-Asp-Gly-Glu-Ser-Asp-Ser-Asp-Ser-Glu-Asp-Ala-Leu) of murine RIIα were synthesized. These regions were chosen because residues 50–62 lie in a variable region of RIIα not conserved between species while residues 68–82 form a conserved acidic region (12). The RII 50–62 peptide did not block RII/MAP2 interaction (Fig. 4 and Table I). However, high concentrations of RII 68–82 peptide (100 μM and above) decreased MAP2 binding 3-fold (Fig. 4 and Table I). A control peptide of similar amino-acid composition to RII 68–82 peptide but different sequence (Lys-Tyr-Ile-Leu-Asp-Asp-Leu-Glu-Pro-Glu-Glu-Leu-Glu-Asp) was unable to block RII/MAP2 interaction in a concentration range from 1 nM to 10 mM (Fig. 4). RII 68–82 peptide can be phosphorylated by casein kinase II but attempts to show ^{32}P phosphopeptide binding to MAP2 were negative.

An RII monomer containing residues 1–14 (Fig. 5*A*) was formed by denaturation of RII and renaturation with excess RII 1–14 peptide to block dimer formation. Monomeric RII did not bind MAP2 while renatured RII dimer retained full binding activity (Fig. 5*B*). This confirms RII dimerization is essential for binding.

Common or Overlapping Anchoring Protein Receptor Sites on RIIα—Once components of the MAP2 receptor were established other RII anchoring proteins were screened to see if they bound the RIIα dimer. In all cases disruption of dimerization destroyed anchoring protein binding (Fig. 6). All RIIα probes were used to screen a 47-kDa RII anchoring fragment from the bovine brain protein P75 (15) yielding identical results as shown for MAP2 (Fig. 2*C*). Competition with excess p75 fragment blocked MAP2 binding to RII and vice versa (data not shown).

DISCUSSION

Two distinct peptide regions in each RII protomer appear to participate in anchoring protein interaction. Anchoring proteins can only interact with the intact RII dimer but other regions distal to the dimerization domain may also participate (Fig. 7). Our data clearly demonstrate that dimerization is required for anchoring protein interaction.

Residues 1–30 represent an independent RIIα dimerization subdomain functional when removed from the remainder of the molecule. Secondary structure predictions (28–30) imply that residues 11–23 of RIIα can form β-sheet. Crystallographic analysis proposes β-sheets often participate in protein/protein contact (28–30). Residues of 1–30 of RIIα are highly conserved in all known RII sequences (12). Since conserved structure often reflects conserved function we believe this region is the complete dimerization domain. These findings extend previous studies which have dissected the dimerization domain from the remainder of the molecule by limited proteolysis at arginine 45 (32).

An acidic cluster between residues 68–82 may represent an additional part of the MAP2 receptor because synthetic peptides to this region decreased binding. Secondary structure predictions postulate residues 68–82 could form α-helix (28). Although acidic residues often favor helix formation, the distribution of negative charges throughout this region (8 of 15 residues) is more likely to destabilize any potential helical structure. Alternatively, these acidic side-chains could form a negatively charged face. Negatively charged faces have been

proposed to form protein/protein contact sites for RNA polymerase II on several mammalian transcription activation factors (33). Interactions are maintained through hydrogen bonding between acidic and hydroxylated amino acids (33). The acidic clusters appear to be lesser components of the MAP2 receptor since high RII 68–82 peptide concentrations were needed to effect MAP2 binding. Experiments are in progress to identify other potential anchoring protein contact sites upstream of residue 68 on each RII protomer.

The anchoring protein receptor is immediately adjacent to the autoinhibitor domain in RIIα (Fig. 7). The Arg-Arg-Val-Ser-Val sequence motif (residues 92–96 in murine RIIα) is believed to provide primary contact site with the dormant catalytic subunit (5). The stoichiometry of RII/MAP2 binding implies that one RIIα dimer binds each MAP2 (Table I). Therefore, each holoenzyme complex can associate with an individual MAP2 molecule. The topology of an anchored holoenzyme complex could place both catalytic subunits in close proximity to MAP2 (Fig. 7). MAP2 is hyperphosphorylated by PKA incorporating up to 11 mol of phosphate (34). This suggests RII-anchoring proteins could be the first available substrates phosphorylated upon C subunit activation. It has been shown most RII-anchoring proteins are PKA substrates and suggested their biological activity may be modulated through phosphorylation (16).

A schematic diagram of the RII-anchoring protein receptor summarizing the information presented in this report is in Fig. 7. The dimerization and acidic clusters are separated by a segment of about 40 residues. This segment includes a 30-residue section (residues 42–72) which is highly variable in all RII sequences (12). Others have suggested the variable segment is a species-specific RII-anchoring protein receptor site (35). We believe that this region may be a bridge between the dimerization subdomain and association domains permitting a customized fit for each RII-binding protein. In RIIβ the putative protein bridge is extended by 16 residues which could explain its 7-fold lower affinity for MAP2 (14).

One limitation of our experimental approach is that much of the data is qualitative in nature. Clearly RIIα dimerization promotes MAP2 interaction and the primary sites of contact are within the first 79 residues of the molecule. Future experiments are planned to construct RIIα chimeras which will allow precise measurement of RIIα affinity for MAP2. A more sensitive assay for RIIα/MAP2 interaction will allow us to quantitate any subtle changes in affinity caused by phosphorylation or further deletion of amino acids.

MAP2 and P150 bind through the same or overlapping sites on RIIα. Recently the RII-binding domains of MAP2 has been identified but no sequence homology to P150 is evident (18, 19). Work is underway to identify other RII anchoring proteins and define their RII-binding domains. This may reveal a consensus RII-anchoring sequence. RIIα and RIIβ each may preferentially bind different anchoring proteins. RIIα and RIIβ interaction with different anchoring proteins may promote differential subcellular localization of the type II kinase isoforms. PKA phosphorylation at defined microenvironments mediated through RII anchoring may be the mechanism through which individual cAMP-mediated events are triggered.

Acknowledgments—We wish to thank colleagues in the Vollum Institute and Oregon Health Sciences University for their critical reading of this manuscript, Dr. Jack Erlichman for providing a manuscript prior to publication, and Wendy Carlton for excellent assistance in typing and proofreading of the manuscript.

REFERENCES

1. Krupinski, J. P., Grancoise, C., Bakalyar, H. A., Tang, W-J., Feinstein, P. G., Orth, K., Slaughter, C., Reed, R. R., and Gilman, A. G. (1989) *Science* **244,** 1558–1564
2. Neer, E., and Clapham, D. (1988) *Nature* **333,** 129–133
3. Taylor, S. S. (1989) *J. Biol. Chem.* **264,** 8443–8446
4. Rubin, C. S., Erlichman, J., and Rosen, O. M. (1972) *J. Biol. Chem.* **247,** 6135–6139
5. Corbin, J. D., Sugden, P. H., Lincoln, T. M., and Keely, S. L. (1977) *J. Biol. Chem.* **252,** 3845–3861
6. Rubin, C. S., Rangel-Aldao, R., Sarkar, D., Erlichman, J., and Fleicher, N. (1979) *J. Biol. Chem.* **254,** 3797–3805
7. Hofmann, F., Beavo, J. A., Bechtel, P. J., and Krebs, E. G. (1975) *J. Biol. Chem.* **250,** 7795–7801
8. Corbin, J. D., Keely, S. L., and Park, C. R. (1975) *J. Biol. Chem.* **250,** 218–225
9. Lee, D. F., Carmichael, D. F., Krebs, E. G., and McKnight, G. S. (1983) *Proc. Natl. Acad. Sci. U. S. A.* **80,** 3608–3612
10. Clegg, C., Cadd, G. A., and McKnight, G. S. (1988) *Proc. Natl. Acad. Sci. U. S. A.* **85,** 3703–3707
11. Jahnsen, T., Hedin, L., Kidd, V. J., Beattie, W. G., Lohmann, S. M., Walter, U., Durica, J., Schulz, T. Z., Schiltz, E., Browner, M., Lawrence, C. B., Goldman, D., Ratoosh, S. L., and Richards, J. S. (1986) *J. Biol. Chem.* **261,** 12352–12361
12. Scott, J. D., Glaccum, M. B., Zoller, M. J., Uhler, M. D., Helfman, D. M., McKnight, G. S., and Krebs, E. G. (1987) *Proc. Natl. Acad. Sci. U. S. A.* **84,** 5192–5196
13. Nigg, E. A., Schafer, G., Hilz, H., and Eppenberger, H. M. (1985) *Cell* **41,** 1039–1051
14. Leiser, M., Rubin, C. S., and Erlichman, J. (1986) *J. Biol. Chem.* **261,** 1904–1908
15. Bergman, D. B., Bhattacharyya, N., and Rubin, C. S. (1988) *J. Biol. Chem.* **264,** 4648–4656
16. Lohmann, S. M., DeCamilli, P., Einig, I., and Walter, U. (1984) *Proc. Natl. Acad. Sci. U. S. A.* **81,** 6723–6727
17. Threurkauf, W. E., and Vallee, R. B. (1982) *J. Biol. Chem.* **257,** 3284–3290
18. Rubino, H. M., Dammerman, M., Shafit-Zagardo, B., and Erlichman, J. (1989) *Neuron* **3,** 631–638
19. Obar, R. A., Dingus, J., Bayley, H., and Vallee, R. B. (1989) *Neuron* **3,** 639–645
20. Vallee, R. B. (1986) *Methods Enzymol.* **134,** 104–115
21. Weber, W., Vogel, C-W., and Hilz, H. (1979) *FEBS Lett.* **99,** 62–66
22. Schlaepfer, D. D., Mehlman, T., Burgess, W. H., and Haigler, H. T. (1987) *Proc. Natl. Acad. Sci. U. S. A.* **84,** 6078–6082
23. Kaplan, R., Jaye, M., Burgess, W. H., Schlaepfer, D. D., and Haigler, H. T. (1988) *J. Biol. Chem.* **263,** 8037–8043
24. Kerlavage, A. R., and Taylor, S. S. (1980) *J. Biol. Chem.* **255,** 8483–8488
25. Sanger, F., Nicklen, S., and Coulson, A. R. (1977) *Proc. Natl. Acad. Sci. U. S. A.* **74,** 5463–5467
26. Laemmli, U. K. (1970) *Nature* **227,** 680–685
27. Towbin, H., Staehlin, T., and Gordon, J. (1979) *Proc. Natl. Acad. Sci. U. S. A.* **76,** 4350–4354
28. Chou, P., and Fasman, G. (1974) *Biochemistry* **13,** 211–222
29. Robinson, B., and Suzuki, E. (1976) *J. Mol. Biol.* **105,** 327–356
30. Millar, S. (1989) *Protein Engin.* **3,** 77–83
31. Weber, W., and Hilz, H. (1979) *Biochem. Biophys. Res. Commun.* **90,** 1073–1081
32. Reimann, E. (1986) *Biochemistry* **25,** 6776–6785
33. Sigler, E. (1987) *Nature* **333,** 210–212
34. Vallee, R. (1980) *Proc. Natl. Acad. Sci. U. S. A.* **77,** 3206–3210
35. Øyen, O., Myklebust, F., Scott, J. D., Hansson, V., and Jahnsen, T. (1989) *FEBS Lett.* **246,** 57–64
36. Horowitz, J., Wasco, W., Leisner, M., and Orr, G. O. (1988) *J. Biol. Chem.* **263,** 2098–2104